Supersonic Flow in the Corner Formed by Two Intersecting Wedges

PAUL KUTLER*
NASA Ames Research Center, Moffett Field, Calif.

Theme

EXPERIMENTALISTS,[1,2] for over a decade, have investigated the supersonic flowfield in the axial corner formed by two intersecting wedges. The understanding and prediction of this type of interference flow is of considerable interest to the designer of high-performance hypersonic aircraft and spacecraft (Space Shuttle Orbiter) because of the high local heating that occurs in this region. Such flows are encountered, for example, at wing-body junctures, at control surface roots, and within supersonic inlets.

Theoretical attempts at modeling the corner flow problem have been made in the past,[3,4] but these employed simplifying or incorrect assumptions and thus resulted in questionable solutions. According to the recent survey paper of Korkegi,[5] "there exists no adequate method of predicting even the inviscid flow structure." In the present paper, a numerical solution for the inviscid corner flow is computed using a second-order accurate shock-capturing technique.[6]

Contents

The structure of the conical flow generated by two intersecting wedges immersed in a supersonic stream is shown in Fig. 1. The shock structure consists of the planar shocks emanating from the leading edge of each wedge (with angles of δ_1 and δ_2), a corner shock that joins the two wedge shocks, and two embedded shocks that stretch from the body to their respective triple points. Stretching between each of the triple points and the axial corner is a slip surface or inviscid shear layer. A vortical singularity (a point with multiple values of entropy) exists at the axial corner of the two wedges. It is generated as a result of the flow passing through different points of the curved embedded and corner shocks and converging at the axial corner.

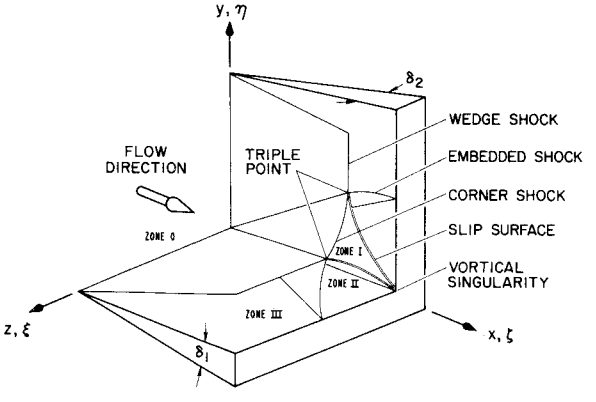

Fig. 1 Coordinate system and typical wave structure.

The regions bounded by the shocks and slip surfaces are denoted as zones 0, I, II, and III (as illustrated in Fig. 1). Zone 0 corresponds to the freestream, and zone III contains simple wedge flow—both having constant flow properties. The flow in zones I and II is rotational because of the convex corner shock and concave embedded shock (viewed from corner). The conical crossflow velocity (the component that results when the total velocity is projected on a sphere whose center is at the origin of the coordinate system) is supersonic in zone III and subsonic in zones I and II. Therefore, the conical problem is mixed elliptic-hyperbolic.

To make the problem totally hyperbolic, the governing partial differential equations (continuity, x, y, and z momentum) in Cartesian space are transformed into nonorthogonal, conical coordinates ($\zeta = x, \eta = y/x$ and $\xi = z/x$; see Fig. 1) and rearranged in conservation-law form to yield the following dimensionless equation:

$$U_\zeta + F_\eta + G_\xi = 0 \tag{1}$$

where

$$U = \zeta^2 \begin{vmatrix} \rho u \\ kp + \rho u^2 \\ \rho uv \\ \rho uw \end{vmatrix}$$

$$F = \zeta \begin{vmatrix} \rho(v - \eta u) \\ \rho u(v - \eta u) - \eta kp \\ \rho v(v - \eta u) + kp \\ \rho w(v - \eta u) \end{vmatrix}$$

$$G = \zeta \begin{vmatrix} \rho(w - \xi u) \\ \rho u(w - \xi u) - \xi kp \\ \rho v(w - \xi u) \\ \rho w(w - \xi u) + kp \end{vmatrix}$$

and where $k = (\gamma - 1)/2\gamma$, γ being the ratio of specific heats.

In Eq. (1), pressure and density are made dimensionless with respect to freestream stagnation conditions and velocity with respect to the maximum adiabatic velocity. The preceding system of equations is made complete by the addition of the energy equation (for constant total enthalpy and a perfect gas) which can be written in the following dimensionless form:

$$p = \rho(1 - u^2 - v^2 - w^2) \tag{2}$$

A rectangular region that completely encompasses the shock structure in the corner is discretized and results in the computational plane shown in Fig. 2. In the η-direction, the lower boundary is the wedge surface, $\eta = \tan\delta_1$, where $j = 1$ (along which the tangency condition is satisfied), while the upper boundary, $j = j_{max}$, is chosen to fall in a region of known flow

Received July 11, 1973; presented as Paper 73-675 at the AIAA 6th Fluid and Plasma Dynamics Conference, Palm Springs, Calif., July 16–18, 1973; synoptic received September 24, 1973; revision received December 7, 1973. Full paper available from AIAA Library, 750 Third Avenue, New York, N.Y. 10017. Price Microfiche, $1.00; hard copy, $5.00. **Order must be accompanied by remittance.**

Index categories: Aircraft Aerodynamics (Including Component Aerodynamics); Supersonic and Hypersonic Flow.

* Research Scientist, Computational Fluid Dynamics Branch. Associate Fellow AIAA.

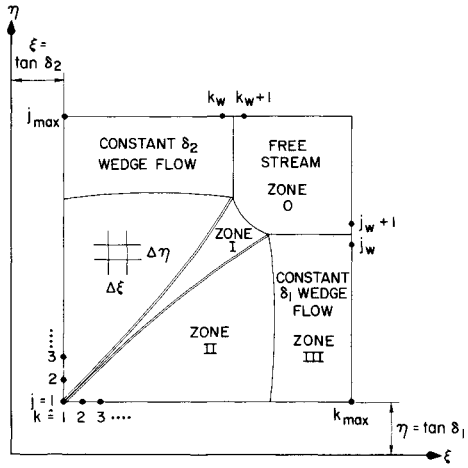

Fig. 2 Computational plane.

properties (well outside the wedge-flow Mach cone from the corner). An analogous procedure is used in the ξ-direction. All interior points are assigned values of the freestream variables initially.

The second-order accurate predictor-corrector scheme devised by MacCormack[7] is used to integrate Eq. (1) iteratively until the term U_ζ is zero, implying the establishment of a conical flowfield. Shock waves and slip surfaces that should exist form automatically and are correctly positioned within the computational network of points in the converged solution.

The most recent published experimental data obtained for the corner flow problem are by West and Korkegi.[2] They tested an equal wedge angle ($\delta_1 = \delta_2 = 9.49°$) configuration in Mach 2.98 flow over a Reynolds number range from 0.4×10^6 to 60×10^6, which included laminar, transitional, and turbulent boundary layers. A numerical solution† for the corresponding inviscid case was obtained, and the shock wave and slip surface structure are compared with the high Reynolds number experiment in Fig. 3.

The inviscid embedded shock is slightly concave when viewed from the origin and falls inside the location of the corresponding

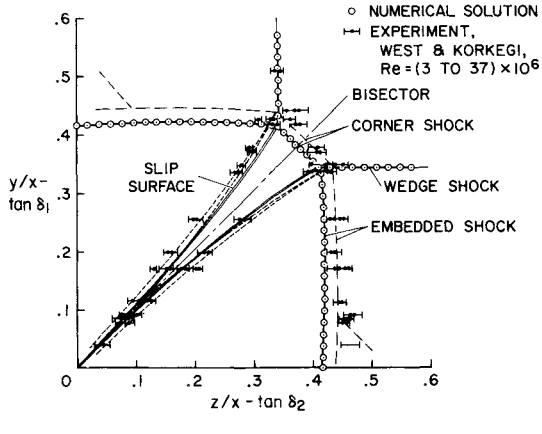

Fig. 3 Comparison of numerical and experimental shock patterns; $M = 2.98$, $\delta_1 = \delta_2 = 9.49°$.

† For the numerical results presented, a 30×30 rectangular grid was used. Each computation, consisting of 400 iterations, required approximately 20 min of CPU time on an IBM 360/67 linked with an IBM 2250 cathode-ray display tube.

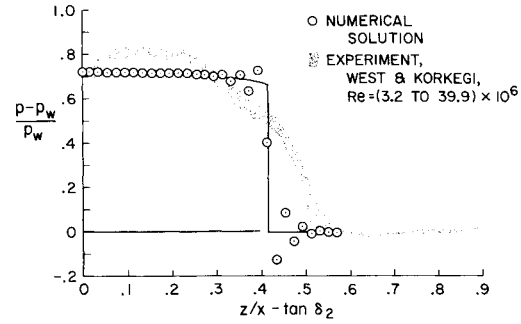

Fig. 4 Comparison of numerical and experimental surface pressure distribution; $M = 2.98$, $\delta_1 = \delta_2 = 9.49°$.

experimental shock. The corner shock, which is slightly convex when viewed from the origin, also falls inside the experimental shock. The position of the experimental and numerical wedge shocks agrees exactly. It appears, therefore, that the displacement effects of the boundary layer in the region bounded by the corner and embedded shocks result in an effective thickening of the body, and this forces the shock structure outward.

The location of the slip surfaces for this case can be found from plots of density and are shown as the thin double line in Fig. 3 stretching from the triple point to the origin. The slip surface is slightly curved and asymptotically approaches the bisector near the origin. The experimental shear layer is also curved but appears to merge before the origin is reached. Since the positions of the numerical and experimental triple points are different, the comparison between the inviscid slip surface and viscous shear layer, which originate at the triple points, is unfair. But, qualitatively, their basic shapes are the same.

A comparison of the numerical and experimental (turbulent boundary layer) surface pressures is shown in Fig. 4. The first pressure rise in the experimental data (decreasing z/x) indicates the onset of separation. This is followed by a reduced gradient region that indicates separation and again a rapid pressure rise that indicates reattachment. The pressure between the reattachment point and the origin is greater than that of the inviscid result. This higher pressure indicates an apparent thickening of the body in this region due to boundary-layer displacement effects.

References

[1] Stainback, P. C., "An Experimental Investigation at a Mach Number of 4.95 of Flow in the Vicinity of a 90° Interior Corner Aligned with the Free-Stream Velocity," TN D-184, 1960, NASA.

[2] West, J. E. and Korkegi, R. H., "Supersonic Interactions in the Corner of Intersecting Wedges at High Reynolds Numbers," *AIAA Journal*, Vol. 10, No. 5, May 1972, pp. 652–656; also ARL 71-0241, 1971, Aerospace Research Labs., Wright-Patterson Air Force Base, Ohio.

[3] Wallace, J. and Clarke, J. H., "Uniformly Valid Second-Order Solution for Supersonic Flow Over Cruciform Surfaces," *AIAA Journal*, Vol. 1, No. 1, Jan. 1963, pp. 179–185.

[4] Goebel, T. P., "A Theoretical Study of Inviscid Supersonic Flow Along a Corner Formed by the Intersection of Two Wedges," Ph.D. thesis, 1969, Univ. of California, Los Angeles, Calif.

[5] Korkegi, R. H., "Survey of Viscous Interactions Associated with High Mach Number Flight," *AIAA Journal*, Vol. 9, No. 5, May 1971, pp. 771–783.

[6] Kutler, P. and Lomax, H., "Shock-Capturing, Finite-Difference Approach to Supersonic Flows," *Journal of Spacecraft and Rockets*, Vol. 8, No. 12, Dec. 1971, pp. 1175–1182.

[7] MacCormack, R. W., "The Effect of Viscosity in Hypervelocity Impact Cratering," AIAA Paper 69-354, Cincinnati, Ohio, 1969.